ACS APPLIED MATERIALS & INTERFACES

Research Article

www.acsami.org

Versatile Microfluidic Platform for the Assessment of Sialic Acid Expression on Cancer Cells Using Quantum Dots with Phenylboronic Acid Tags

Jun-Tao Cao,[†,‡] Peng-Hui Zhang,[‡] Yan-Ming Liu,[†] E. S. Abdel-Halim,[§] and Jun-Jie Zhu*[,‡]

[†]College of Chemistry and Chemical Engineering, Xinyang Normal University, Xinyang 464000, People's Republic of China

[‡]State Key Laboratory of Analytical Chemistry for Life Science, School of Chemistry and Chemical Engineering, Nanjing University, Nanjing 210093, People's Republic of China

[§]Petrochemical Research Chair, Chemistry Department, College of Science, King Saud University, P.O. Box 2455, Riyadh 11451, Saudi Arabia

ABSTRACT: This work describes a versatile microfluidic platform for evaluation of cell-surface glycan expression at the single-cell level using quantum dots (QDs) tagged with phenylboronic acid. The platform was integrated with dual microwell arrays, allowing the introduction of cells in two states using the same cell culture chamber. The simultaneous analysis of cells in the same environment minimized errors resulting from different culture conditions. As proof-of-concept, the expressions of sialic acid (SA) groups on K562 cells, with or without 3′-azido-3′-deoxythymidine (AZT) treatment, were evaluated in the same chamber. 3-Aminophenylboronic acid functionalized CdSeTe@ZnS-SiO_2 QDs (APBA-QDs) were prepared as probes to recognize SA groups on K562 cells with only one-step labeling. The results showed that the expression of SA moieties on K562 cells was increased by 18% and 31% after treatment with 20 and 40 μM AZT, respectively. Performing the drug treatment and control experiments simultaneously in the same chamber significantly improved the robustness and effectiveness of the assay. The strategy presented here provides an alternative tool for glycan analysis in a sensitive, high-throughput, and effective manner.

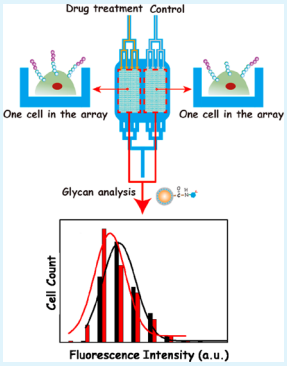

KEYWORDS: *microfluidic platform, dual microwell array, QDs-APBA, sialic acid, K562 cells*

INTRODUCTION

Cell-surface glycans play essential roles in a variety of cellular processes including differentiation, proliferation, immune recognition/response, intercellular signaling, and pathological processes.[1] Full understanding of glycoproteomics and the biological roles of glycoconjugates requires effective tools to identify cell-surface glycan expression. Although methods such as mass spectrometry and chromatography have been developed for glycan analysis,[2,3] these approaches are destructive and not suitable for living cell interrogation. The use of lectins or antibodies as recognizing elements provides a nondestructive method to evaluate cell-surface glycans.[4,5] The current fluorescence-based lectin arrays[6,7] and probe-tagged lectin-based electrochemical strategies perform well in glycan profiling,[8,9] but the information obtained by these methods is the average outcome from a population of cells.

To avoid the loss of information associated with cellular heterogeneity, microfluidic-chip-based high-throughput single-cell analysis has the potential to analyze a large quantity of individual cells to determine a distribution of responses.[10] The technique has been validated in biological models such as membrane protein detection,[11] a single-cell cytotoxicity assay,[12] digital polymerase chain reaction analysis,[13,14] and whole-transcriptome sequencing.[15] Among various microfluidic methods for single-cell analysis, microfluidic-based arrays have attracted great attention for their advantages including facile manipulation, high-throughput capability, and low cell sample consumption.[16−19]

Recently, our group developed a microfluidic device integrated with a microwell array for high-throughput profiling of cell-surface glycan expression using a quantum dot (QD)-based immunofluorescence (IF) approach.[20] The QD-based indirect IF staining protocol was highly sensitive because QDs have high brightness and resistance to photobleaching. Although the method had many distinct advantages for glycan analysis, the drug treatment and control experiments were performed on two separate chips leading to a long assay time. Moreover, the multiple washing steps in the IF staining process were time-consuming. To simplify the staining process, Liu et al.[21] reported a new class of imaging probes based on QDs with small molecule phenylboronic acid (PBA) tags for highly specific and efficient labeling of sialic acid (SA) on living cells. Their results showed that the probes enabled one-step labeling and continuous tracking. By combining this type of probe with glyconanoparticles, Han et al.[22] proposed an amplification strategy for fluorescent analysis of dynamic glycan expression

Received: April 23, 2015
Accepted: June 18, 2015
Published: June 18, 2015

DOI: 10.1021/acsami.5b03519
ACS Appl. Mater. Interfaces 2015, 7, 14878−14884

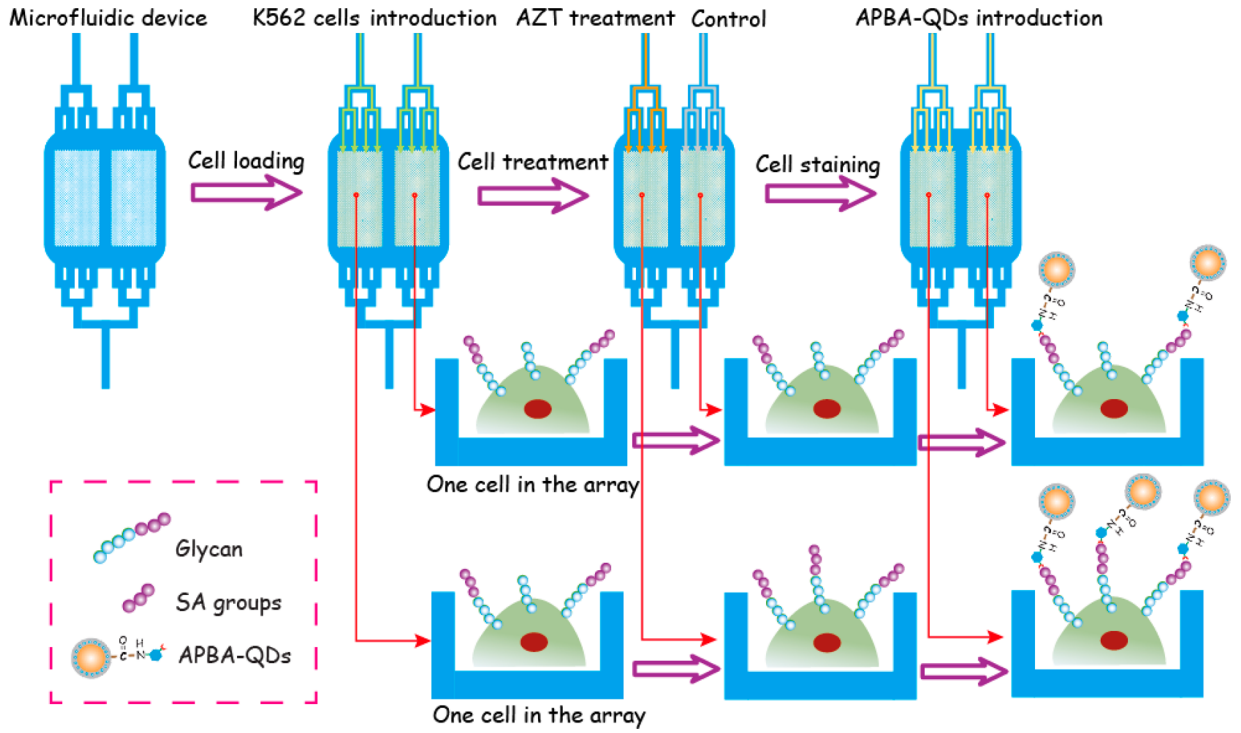

Figure 1. Schematic illustration of the microfluidic platform for glycan profiling on K562 cells in response to AZT.

on living cells. These interesting protocols combined with a microfluidic technique may provide a novel strategy for the construction of a glycan evaluation platform.

Herein, we have integrated dual microwell arrays on the microfluidic chip to develop a versatile single-cell microfluidic platform for SA analysis using QDs labeled with 3-aminophenylboronic acid (APBA). The platform allowed trapping of two different cell lines in one cell culture chamber and treating cells selectively by controlling laminar flow in the microenvironment. The CdSeTe@ZnS-SiO_2 QDs functionalized with APBA tags (APBA-QDs) were prepared for specific and efficient labeling of SA on the cell surface. By combining the microfluidic platform with these sensitive and specific APBA-QDs, glycan expression and changes after drug treatment could be measured on a single K562 cell simultaneously.

EXPERIMENTAL SECTION

Reagents. Reduced glutathione (GSH, 99%) was purchased from Aladdin Chemistry (Shanghai, China). Tetraethylorthosilicate (TEOS) was obtained from Sinopharm Chemical Reagent Co. (Shanghai, China). Zinc acetate ($Zn(OAc)_2$) was from Shanghai Meixing Chemical Co. (Shanghai, China). Rhodamine B, 3′-azido-3′-deoxythymidine (AZT), APBA, and 1-ethyl-3-(3-(dimethylamino)-propyl) carbodiimide (EDC) were from Sigma−Aldrich Inc. (St Louis, MO, USA). Calcein-AM and Hoechst 33342 were from Dojindo Laboratories (Kumamoto, Japan). Fluorescein isothiocyanate conjugated *Sambucus nigra* agglutinin (FITC-SNA) was purchased from Vector Laboratories (Burlingame, CA, USA). Phosphate-buffered saline (PBS, pH 7.4) contained 137 mM NaCl, 2.7 mM KCl, 87 mM Na_2HPO_4, and 14 mM KH_2PO_4. All aqueous solutions were prepared using ultrapure water (Milli-Q, Millipore, Billerica, MA, USA).

Apparatus. UV−visible (UV−vis) absorption spectra were obtained using a UV-3600 spectrophotometer (Shimadzu, Tokyo, Japan). Fluorescence measurements were carried out using a Bruker RF-5301PC fluorescence spectrometer. Fourier-transform infrared (FTIR) spectroscopic measurements were performed on a Bruker model VECTOR22 Fourier-transform spectrometer using KBr pressed disks.

Preparation of APBA-QDs. The preparation of CdSeTe@ZnS-SiO_2 quantum dots followed our previous report, and the concentration of the QDs was about 600 nM.[23] The APBA-functionalized CdSeTe@ZnS-SiO_2 was synthesized as follows. First, 450 μL of APBA (2 mM) was mixed with 50 μL of EDC (3 mg mL^{-1}). The solution was cooled in an ice bath and treated with 500 μL of CdSeTe@ZnS-SiO_2 QD solution (0.05 μM). The reaction was kept at 0 °C for 4 h. The reaction mixture was ultrafiltered to remove free APBA, and the obtained conjugates were washed three times with water by ultrafiltration to obtain APBA-QDs. The obtained APBA-QDs were stored at 4 °C prior to use.

Device Fabrication. The microfluidic device was fabricated using a standard soft lithography method.[24,25] Two negative photoresist SU-8 (Microchem, Newton, CA, USA) based molds were used to generate the dual microwells and the microfluidic channels. The molds of the dual microwell arrays and the fluidic layer were fabricated using SU-8 photoresist. The fluidic layer and the microwell array layer were made by pouring polydimethylsiloxane (PDMS, 10:1 elastomer to cross-linker ratio) onto their molds to a thickness of 2 mm and curing at 70 °C for 2 h. The cured layers were peeled from the mold carefully. The fluidic layer consisted of a cell culture chamber and flow channels with a height of 60 μm. The microwell layer integrated two microarrays, and each array contained 560 microwells. The distance between the right edge of the left array and the left edge of the right array was 500 μm. The diameter of each microwell was 30 μm, and the microwell depth and interwell distance (edge to edge) were fixed at 25 and 15 μm, respectively. After the two PDMS layers were treated with air plasma (Harrick Scientific Corporation, Ossining, NY, USA), the microchannel layer was aligned over the microwell layer under an optical microscope. Methanol was used as a lubricant to facilitate the alignment.[25] Finally, the device was bonded at 45 °C for 15 min and then at 70 °C for 1 h. The schematic diagram of the overall microfluidic device is shown in Figure 1.

Cell Culture. K562 chronic myelogenous leukemia and NIH-3T3 mouse fibroblast cell lines were obtained from Nanjing KeyGen Biotech Co., Ltd. (Nanjing, China). K562 cells were cultured in RPMI 1640 medium (Gibco, Grand Island, NY, USA) containing 10% fetal

DOI: 10.1021/acsami.5b03519
ACS Appl. Mater. Interfaces 2015, 7, 14878−14884

calf serum (HyClone, Logan, UT, USA), 100 units mL^{-1} penicillin, and 100 μg mL^{-1} streptomycin at 37 °C in a humidified incubator containing 5% CO_2. NIH-3T3 cells were harvested from 90% confluent cell culture plates. K562 cells were obtained at the logarithmic growth phase. The cell density was determined using a Petroff–Hausser cell counter.

Chip Loading. Prior to use, the microfluidic chip was primed with 75% ethanol (v/v) and vacuumized to wet and sterilize the device. After rinsing with 0.01 M PBS (pH 7.4) for 3 min, the device was treated with 2% bovine serum albumin (BSA) in PBS at 37 °C for 30 min to block the microwell array surface.

For one-cell-type loading, the same volumes of cell suspensions were introduced through the two inlets of the device simultaneously, allowing the cells to flow from up to down the microwell arrays by hydrogravity. Subsequently, by equalizing the inlet and outlet volumes with PBS, the flow was halted allowing the cells to settle into the microwells by gravitational force. The flow was then reversed by introducing a drop of PBS into the outlet. The cells in the outlet passed through the microwell regions to allow more cells into the microwells. This process was repeated twice or more to achieve a satisfied single-cell occupancy (about 65% for K562 cells). Finally, the cell samples in the inlet were gently aspirated out, and extra PBS medium was immediately introduced into the inlets to remove residual cells between the microwells in the microchamber.

For loading of two different cell types, the trapping process was modified from the aforementioned description. Equal volumes of PBS and cell A suspension were introduced into the two inlets. The cell A suspension flowed up to down one of the microwell arrays and did not migrate to the other array due to the effect of laminar flow. Satisfactory single-cell occupancy (about 60% for K562 cells) was obtained by introducing the same volumes of PBS and cell A suspension to the two inlets continuously. The cells flowing into the outlet were gently aspirated, and a certain volume of PBS was added into the outlet (the volume of liquid in the outlet was less than those in the two inlets). Cells in the inlet were then gently aspirated out, and an appropriate amount of PBS was added into the inlet. The cell B suspension was introduced into the other inlet, and the volume of the cell B suspension was equal to that of PBS. The trapping process was repeated as for cell A until satisfactory single-cell occupancy was obtained for cell B (about 56% for NIH-3T3 cells). This resulted in cell A and cell B being trapped in separate arrays within the same microchamber.

Staining of Microfluidic APBA-QDs for Glycan Analysis. Glycan analysis of a single cell line with APBA-QDs was performed on the microfluidic platform using K562 cells as a model (shown in Figure 1). After cell loading, culture media with and without AZT (20 or 40 μM) in the same volume were introduced into the two inlets of the chip, respectively. Because of the laminar flow in the microchamber, the K562 cells on one microwell array were exposed to culture medium containing AZT, while the cells on the other array were exposed to culture medium without drug. After incubation at 37 °C for 3 h, the cells were washed with PBS and subsequently fixed with 4% w/w paraformaldehyde solution in PBS at 25 °C for 10 min. Finally, APBA-QDs were introduced into the device for cell staining.

Microscopy Imaging and Data Analysis. Phase-contrast and fluorescence images were acquired using a Nikon TE2000-U inverted fluorescent microscope equipped with a cooled CCD camera (DS-U1, Nikon Corporation, Japan). Fluorescent images were analyzed using Nikon NIS Elements imaging software (Nikon Corporation, Japan). The average fluorescence intensity of each cell region was corrected by subtracting the average local background fluorescence of the empty wells in the array.

Flow Cytometric Analysis of Glycan Expression on K562 Cells. K562 cells were treated with or without AZT (20 or 40 μM) for 3 h. After being collected by centrifugation and washed with cold PBS buffer, the cells were resuspended in 0.01 M PBS at pH 7.4. The cell concentration was determined. Then, 50 μL of 1×10^7 cells mL^{-1} cell suspension was added to 450 μL of PBS containing 20 μg mL^{-1} FITC-SNA, 1 mM Mn^{2+}, and 1 mM Ca^{2+} at room temperature. After incubation for 30 min at room temperature, the cells were collected by centrifugation, washed with PBS, resuspended in 500 μL of PBS, and assayed by flow cytometry (Becton Dickinson, Franklin Lakes, NJ, USA). Unlabeled K562 cells were used as the negative control for estimation of autofluorescence.

RESULTS AND DISCUSSION

Preparation and Characterization of APBA-QDs. QDs have attracted increasing interest as fluorescent probes due to their photostability, continuous absorption spectra, and efficient and tunable emission. CdSeTe@ZnS-SiO_2 QDs were prepared as the fluorescent probe.[23] The QDs exhibited ultrahigh

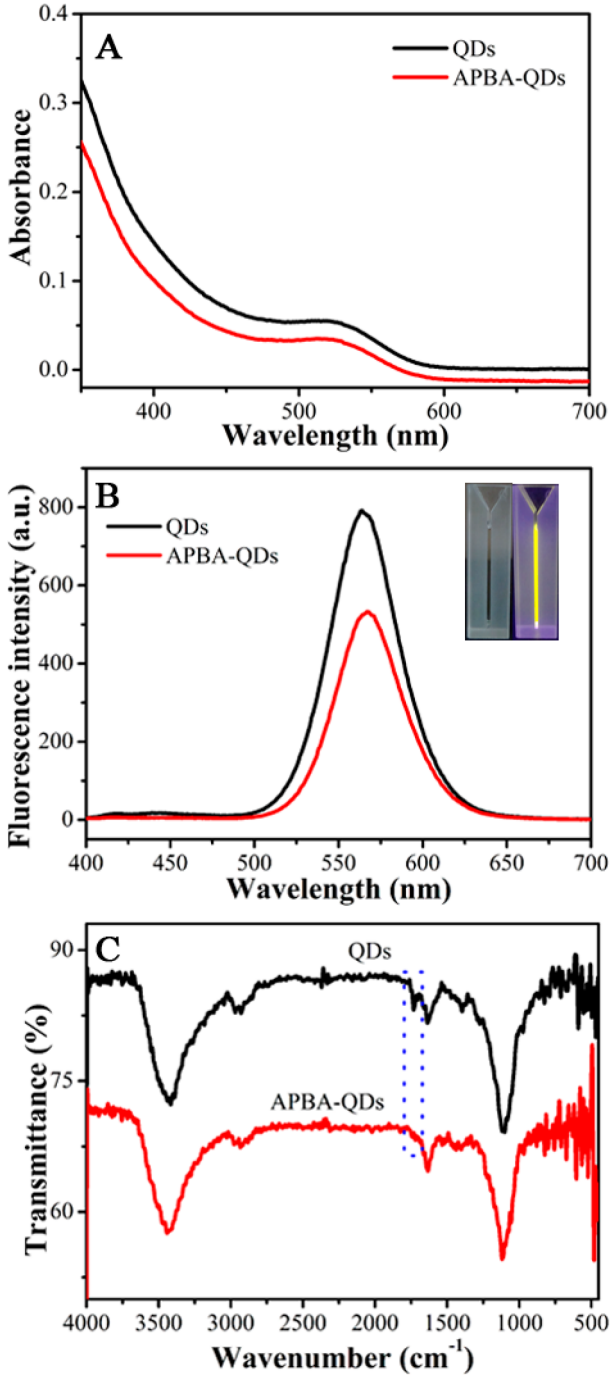

Figure 2. (A) UV–vis, (B) fluorescence, and (C) FTIR spectra of CdSeTe@ZnS-SiO_2 QDs and APBA-QDs. Insets in panel B are images of APBA-QDs taken under natural and UV light.

DOI: 10.1021/acsami.5b03519
ACS Appl. Mater. Interfaces 2015, 7, 14878–14884

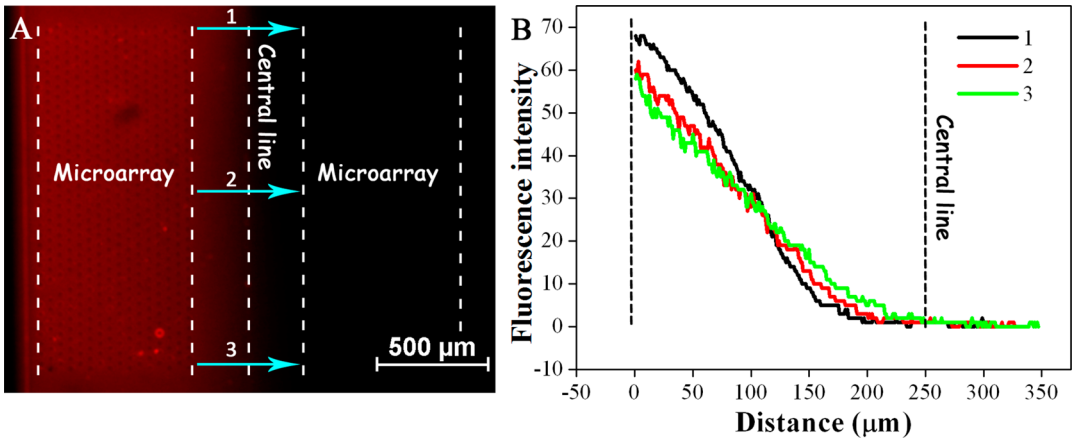

Figure 3. Laminar flow in the microchamber. (A) Fluorescence image of the chamber. The same volumes of RhoB (1 μg mL^{-1}) and PBS (10 mM) were introduced into each array. Scale bar, 500 μm. (B) Fluorescence intensity profiles at three different positions within the chamber, corresponding to positions 1−3 in panel A.

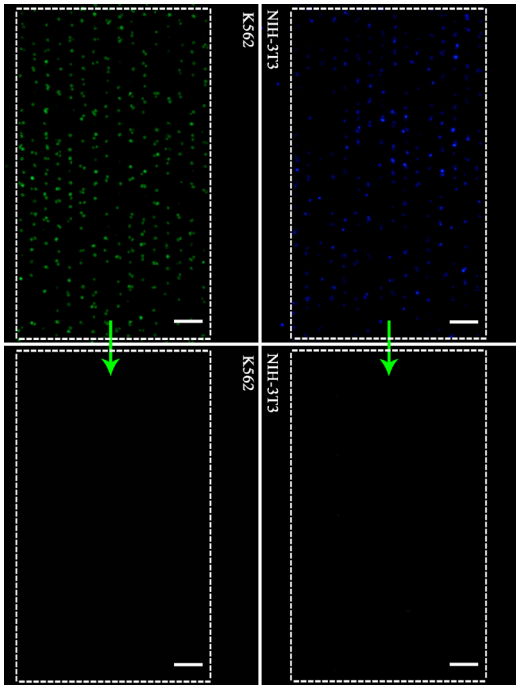

Figure 4. Fluorescence micrograph of K562 (green) and NIH-3T3 (blue). K562 and NIH-3T3 cells were prestained with calcein-AM and Hoechst 33342, respectively, before introduction into the device. The arrays containing K562 cells and NIH-3T3 cells were excited by UV and blue light, respectively.

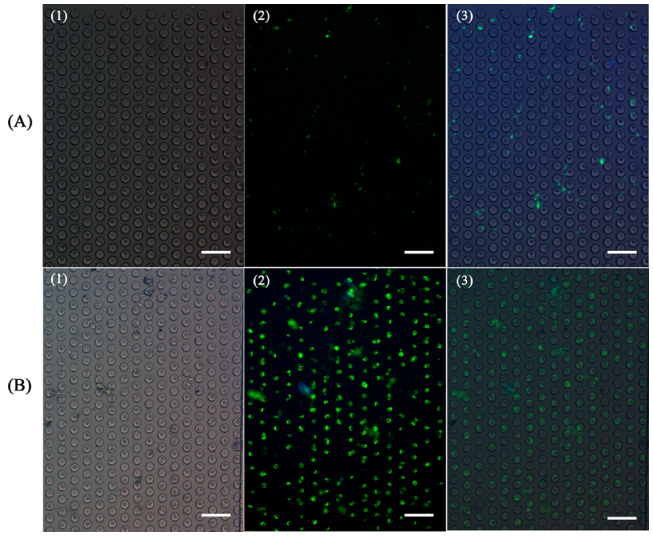

Figure 5. Images of K562 cells treated with (A) QDs for 10 min and then (B) APBA-QDs for 5 min. (1) Bright-field images, (2) fluorescence images (0.5 s exposure), (3) overlay of the corresponding fluorescence image and bright-field image. Cells were prefixed, and the chamber was rinsed after introduction of QDs or APBA-QDs. Scale bars, 100 μm.

quantum yield, low toxicity, and excellent photostability, all of which are beneficial for their application in cell biology. To introduce PBA ligands, APBA was covalently linked to carboxylic acid groups on the CdSeTe@ZnS-SiO_2 QDs through EDC coupling. As shown in Figure 2A, B, the UV−vis and fluorescence spectra (absorption profile, emission wavelength) of the functionalized QDs (APBA-QDs) showed little change after reaction, in accordance with a previous report.[21] Although the quantum yield of the QDs decreased after reaction (Figure 2B), the as-prepared APBA-QDs met the requirements for sensitive cell-surface glycan profiling. Successful synthesis of the APBA-QDs was confirmed by FTIR spectra (Figure 2C). In comparison with the FTIR spectrum of the starting QDs, the peak corresponding to carboxylic acid (−COOH) at 1728 cm^{-1} disappeared in the FTIR spectrum of APBA-QDs, while the signal at 1578 cm^{-1} corresponding to amide groups (−CONH−) appeared. These results are similar to the phenomenon observed by Wu et al.,[26] confirming the formation of APBA-QDs.

Chip Design. By using conventional methods, it is difficult to analyze single cells under different chemical stimuli on the same culture platform. Differences in the culture conditions may cause significant errors. To address this problem, we designed a microfluidic device with dual microwell arrays. In this device, a flow layer with flow channels and cell culture chambers was used for reagent introduction, laminar flow formation, and cell culture. The dual microwell array enabled the entrapment of two sets of the same cell type or two different cell types. By using this device, the same cell type could be introduced into the dual microarray to obtain two single-cell arrays. The culture medium, with or without drug, could flow through the two arrays in the chamber separately,

DOI: 10.1021/acsami.5b03519
ACS Appl. Mater. Interfaces 2015, 7, 14878−14884

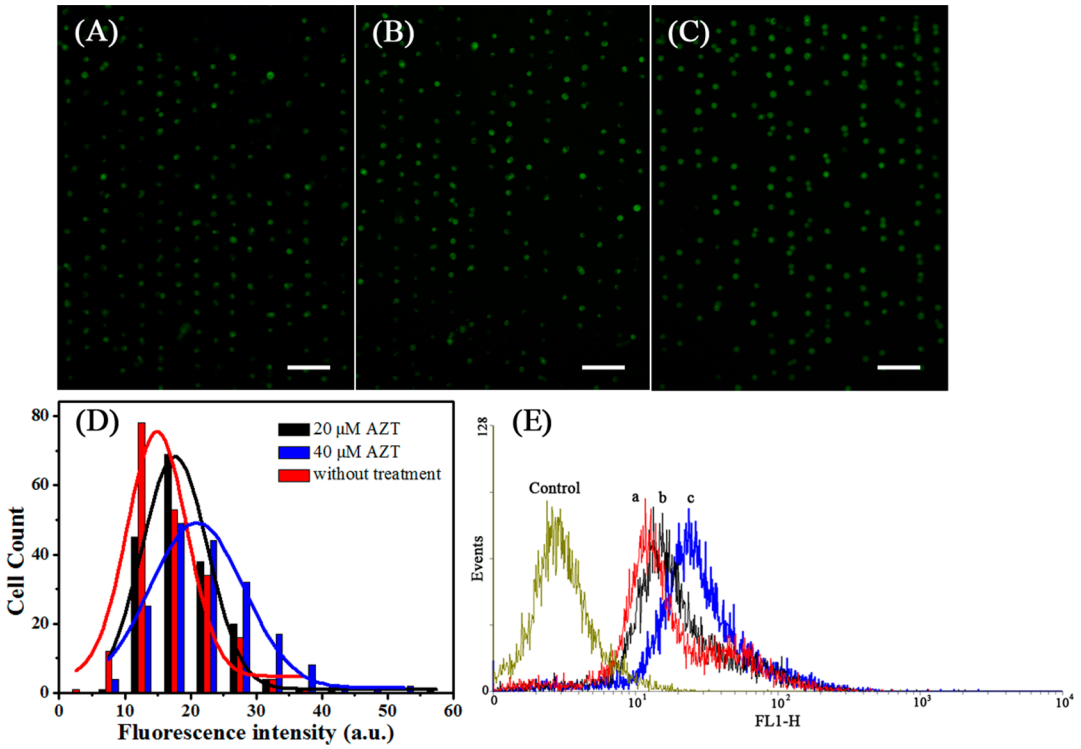

Figure 6. Fluorescence images of cells on a chip (A) untreated or treated with (B) 20 μM or (C) 40 μM AZT. Exposure time, 0.25 s. Scale bar, 100 μm. (D) Histogram of the predicted average fluorescence intensity of a single cell, untreated and after treatment with AZT. (E) Fluorescence profile of K562 cells with or without AZT treatment. K562 cells (a) untreated or treated with (b) 20 μM or (c) 40 μM AZT for 3 h, and the appearance of the surface fluorescence was monitored by flow cytometry using FITC-SNA.

controlled by laminar flow. Consequently, one array could be exposed to culture medium with drug, while the other array was exposed to culture medium without drug as a control group. The simultaneous analysis of drug-treated and control cells in the same chamber significantly improved the robustness and effectiveness of the assay. Additionally, different cell types could be introduced into the separate array within the chamber. Coculture of two different cell types could be realized, and the glycan expression of the different cell types could be analyzed simultaneously.

Laminar Flow Control in the Chamber. Interdiffusion and interfacial stabilities at the two-stream interface were evaluated by the introduction of RhoB into one of the streams in the fluidic channel. A flow rate of 25 μL min^{-1} was used to perfuse the channels. The dye intensity profile across the flow channel was measured at three different positions in the chamber corresponding to positions 1−3 in Figure 3A. The results showed that the fluorescence intensity of the dye dropped to background levels at the central line of the arrays along the entire measured region (Figure 3B), indicating that interdiffusion of the two streams had a negligible influence on subsequent analyses. The stability of the interface between the two streams was examined by monitoring the movement of the interface with time. The variation of the interface was less than 10 μm during a 3 h recording period.

Cell Loading in the Microfluidic Dual Arrays. For loading of the same cell type, the trapping process was easily completed. Unlike loading of the same cell type, the flow direction of the cell suspension cannot be reversed when trapping two different cell types. Therefore, the laminar flow must be accurately controlled for loading of different cell types into the designated microarray. To distinguish cells in the microarray, K562 and NIH-3T3 cells were prestained with calcein-AM and Hoechst 33342, respectively, before being introduced into the device. After loading, fluorescence images were taken under UV and blue light, respectively, as shown in Figure 4. It can be seen that the calcein-AM treated K562 cells with green fluorescence and NIH-3T3 cells with blue fluorescence are well isolated into two different regions. Thus, loading of two different cell lines onto separate arrays in the same cell culture chamber was achieved.

Receptor Specificity. Several recent reports have demonstrated that PBA prefers to bind with SA on cell surfaces,[21,22,26−28] providing an innovative molecular recognition platform for profiling SA on living cells. To verify the specificity of the interaction of PBA ligands with cell-surface SA receptors, the cells were treated with QDs and APBA-QDs, respectively. The cells trapped in the wells were prefixed with 4% w/w paraformaldehyde solution for 10 min. After fixation, the cells were rinsed with PBS for 10 min and 2% BSA for 30 min to block nonspecific binding sites on the cell surface. As shown in Figure 5, the introduction of QDs for 10 min did not lead to overtly detectable labeling. The observed faint fluorescence is likely due to nonspecific adsorption of QDs on the surface of the microwell array. After rinsing with PBS for 5 min, APBA-QDs were introduced into the platform, and the cells were stained to produce high brightness within 5 min. The staining observed was attributed to the specific recognition of APBA by the SA receptors on the cell surface, demonstrating the effective labeling performance of the present strategy and its suitability for high-throughput analysis of SA groups on single cells.

Evaluation of Glycan Expression on Cells in Response to AZT. Previous studies have shown that the intracellular

DOI: 10.1021/acsami.5b03519
ACS Appl. Mater. Interfaces 2015, 7, 14878−14884

metabolite of AZT can inhibit nucleotide sugar transport and thus significantly modify the glycosylation of protein and lipids.[29,30] To further investigate the performance of the present method for glycosylation profiling, the SA moieties on individual K562 cells treated with or without AZT were evaluated in the same microchamber simultaneously. With the laminar flow formed in the chamber, the K562 cells located in one array were exposed to the culture medium containing AZT, whereas the cells located in the other array were exposed to the culture medium alone. By using this strategy, the effects of different concentrations of AZT exposure (20 or 40 μM) on the expression of SA moieties by individual K562 cells are shown in Figure 6. Compared to the untreated cells in Figure 6A, the fluorescence intensity of the cells increased with AZT treatment (Figure 6B, C). The increase of fluorescence reflects an enhanced expression of SA moieties on the surface of cells treated with AZT. The total cell numbers for each fluorescence image were about 250 ± 30 (all cells in the image). In the quantitative analysis, only the microwells with an individual cell (about 200 ± 20 cells) were measured using fluorescence microscopy in Figure 6A–C. The wells with two or three cells were not included in the quantitative study. Fitting each individual cell fluorescence response yields a histogram of the fluorescence distribution for treated and untreated cells (Figure 6D). The expression of SA moieties on K562 cells was increased by 18% and 31% after treatment with 20 and 40 μM AZT, respectively. The changes of the SA moieties on K562 cells were also confirmed by flow cytometric analysis on the basis of the specific recognition between SNA and SA on the cell surface[8] (Figure 6E). The glycan expression status on the cell surface was consistent with the results from the microfluidic-chip-based method; both demonstrated that the SA moieties on the cell surface increased after AZT exposure and the increase exhibited a dose-dependent manner.

CONCLUSIONS

A versatile microfluidic platform with dual microwell arrays was constructed for the evaluation of glycan expression on a single cell using APBA-QDs as the fluorescence probe. The platform allowed profiling of glycan expression on two different cell lines or performing drug treatment and control experiments on the same cell lines in the same chamber. Glycan expression and responses to chemical stimuli could be profiled at the single-cell level with rare cell samples. Coupled with the microfluidic platform, CdSeTe@ZnS-SiO_2 QDs functionalized with PBA provide sensitive and specific recognition of SA on the cell surface with only one-step labeling. This approach will not only be useful for studies aimed at rapid labeling and identification of SA moieties at the single -cell level required for glycoproteomics but also for effective monitoring and tracking of cell-surface glycans in response to chemical stimuli.

AUTHOR INFORMATION

Corresponding Author

* Phone/Fax: (86)2583597204; e-mail: jjzhu@nju.edu.cn.

Notes

The authors declare no competing financial interest.

ACKNOWLEDGMENTS

This research was financially supported by the National Basic Research Program of China (2011CB933502), National Natural Science Foundation of China (grant nos. 21335004, 21375114, and 21405129) and State Key Laboratory of Analytical Chemistry for Life Science (SKLACLS1419). The authors extend their appreciation to the Deanship of Scientific Research at King Saud University for funding the work through the research group project no. RGP-VPP-029.

REFERENCES

(1) Raman, R.; Raguram, S.; Venkataraman, G.; Paulson, J. C.; Sasisekharan, R. Glycomics: An Integrated Systems Approach to Structure-Function Relationships of Glycans. *Nat. Methods* **2005**, *2*, 817–824.

(2) Yang, S.; Yuan, W.; Yang, W. M.; Zhou, J. Y.; Harlan, R.; Edwards, J.; Li, S. W.; Zhang, H. Glycan Analysis by Isobaric Aldehyde Reactive Tags and Mass Spectrometry. *Anal. Chem.* **2013**, *85*, 8188–8195.

(3) Melmer, M.; Stangler, T.; Premstaller, A.; Lindner, W. Comparison of Hydrophilic-Interaction, Reversed-Phase and Porous Graphitic Carbon Chromatography for Glycan Analysis. *J. Chromatogr. A* **2011**, *1218*, 118–123.

(4) Lis, H.; Sharon, N. Lectins: Carbohydrate-Specific Proteins That Mediate Cellular Recognition. *Chem. Rev.* **1998**, *98*, 637–674.

(5) Agard, N. J.; Bertozzi, C. R. Chemical Approaches to Perturb, Profile, and Perceive Glycans. *Acc. Chem. Res.* **2009**, *42*, 788–797.

(6) Jeong, H.; Kim, Y. G.; Jang, S. C.; Yi, H.; Lee, C. S. Profiling Surface Glycans on Live Cells and Tissues Using Quantum Dot-Lectin Nanoconjugates. *Lab Chip* **2012**, *12*, 3290–3295.

(7) Fry, S. A.; Afrough, B.; Lomax-Browne, H. J.; Timms, J. F.; Velentzis, L. S.; Leathem, A. J. Lectin Microarray Profiling of Metastatic Breast Cancers. *Glycobiology* **2011**, *21*, 1060–1070.

(8) Zhang, X.; Teng, Y.; Fu, Y.; Xu, L.; Zhang, S.; He, B.; Wang, C.; Zhang, W. Lectin-Based Biosensor Strategy for Electrochemical Assay of Glycan Expression on Living Cancer Cells. *Anal. Chem.* **2010**, *82*, 9455–9460.

(9) Ding, L.; Cheng, W.; Wang, X.; Ding, S.; Ju, H. X. Carbohydrate Monolayer Strategy for Electrochemical Assay of Cell Surface Carbohydrate. *J. Am. Chem. Soc.* **2008**, *130*, 7224–7225.

(10) Yin, H.; Marshall, D. Microfluidics for Single Cell Analysis. *Curr. Opin. Biotechnol.* **2012**, *23*, 110–119.

(11) Li, L.; Wang, Q.; Feng, J.; Tong, L. L.; Tang, B. Highly Sensitive and Homogeneous Detection of Membrane Protein on a Single Living Cell by Aptamer and Nicking Enzyme Assisted Signal Amplification Based on Microfluidic Droplets. *Anal. Chem.* **2014**, *86*, 5101–5107.

(12) Hosokawa, M.; Hayashi, T.; Mori, T.; Yoshino, T.; Nakasono, S.; Matsunaga, T. Microfluidic Device with Chemical Gradient for Single-Cell Cytotoxicity Assays. *Anal. Chem.* **2011**, *83*, 3648–3654.

(13) White, A. K.; Heyries, K. A.; Doolin, C.; VanInsberghe, M.; Hansen, C. L. High-Throughput Microfluidic Single-Cell Digital Polymerase Chain Reaction. *Anal. Chem.* **2013**, *85*, 7182–7190.

(14) Thompson, A. M.; Gansen, A.; Paguirigan, A. L.; Kreutz, J. E.; Radich, J. P.; Chiu, D. T. Self-Digitization Microfluidic Chip for Absolute Quantification of mRNA in Single Cells. *Anal. Chem.* **2014**, *86*, 12308–12314.

(15) Streets, A. M.; Zhang, X.; Cao, C.; Pang, Y.; Wu, X.; Xiong, L.; Yang, L.; Fu, Y.; Zhao, L.; Tang, F.; Huang, Y. Microfluidic Single-Cell Whole-Transcriptome Sequencing. *Proc. Natl. Acad. Sci. U.S.A.* **2014**, *111*, 7048–7053.

(16) Carlo, D. D.; Aghdam, N.; Lee, L. P. Single-Cell Enzyme Concentrations, Kinetics, and Inhibition Analysis Using High-Density Hydrodynamic Cell Isolation Arrays. *Anal. Chem.* **2006**, *78*, 4925–4930.

(17) Wlodkowic, D.; Faley, S.; Zagnoni, M.; Wikswo, J. P.; Cooper, J. M. Microfluidic Single-Cell Array Cytometry for the Analysis of Tumor Apoptosis. *Anal. Chem.* **2009**, *81*, 5517–5523.

(18) Figueroa, X. A.; Cooksey, G. A.; Votaw, S. V.; Horowitz, L. F.; Folch, A. Large-Scale Investigation of the Olfactory Receptor Space Using a Microfluidic Microwell Array. *Lab Chip* **2010**, *10*, 1120–1127.

DOI: 10.1021/acsami.5b03519
ACS Appl. Mater. Interfaces 2015, 7, 14878–14884

(19) Hosokawa, M.; Hayashi, T.; Mori, T.; Yoshino, T.; Nakasono, S.; Matsunaga, T. Microfluidic Device with Chemical Gradient for Single-Cell Cytotoxicity Assays. *Anal. Chem.* **2011**, *83*, 3648−3654.
(20) Cao, J. T.; Chen, Z. X.; Hao, X. Y.; Zhang, P. H.; Zhu, J. J. Quantum Dots-Based Immunofluorescent Microfluidic Chip for the Analysis of Glycan Expression at Single-Cells. *Anal. Chem.* **2012**, *84*, 10097−10104.
(21) Liu, A.; Peng, S.; Soo, J. C.; Kuang, M.; Chen, P.; Duan, H. Quantum Dots with Phenylboronic Acid Tags for Specific Labeling of Sialic Acids on Living Cells. *Anal. Chem.* **2011**, *83*, 1124−1130.
(22) Han, E.; Ding, L.; Ju, H. Highly Sensitive Fluorescent Analysis of Dynamic Glycan Expression on Living Cells Using Glyconanoparticles and Functionalized Quantum Dots. *Anal. Chem.* **2011**, *83*, 7006−7012.
(23) Shen, Y.; Li, L.; Lu, Q.; Ji, J.; Fei, R.; Zhang, J.; Abdel-Halim, E. S.; Zhu, J. J. Microwave-Assisted Synthesis of Highly Luminescent CdSeTe@ ZnS-SiO_2 Quantum Dots and Their Application in the Detection of Cu (II). *Chem. Commun.* **2012**, *48*, 2222−2224.
(24) Xia, Y.; Whitesides, G. M. Soft Lithography. *Angew. Chem., Int. Ed.* **1998**, *37*, 550−575.
(25) Herold, K. E.; Avraham, R. *Lab on a Chip Technology*; Caister Academic Press: Norfolk, England, 2009; Vol. *1*.
(26) Wu, W.; Zhou, T.; Berliner, A.; Banerjee, P.; Zhou, S. Glucose-Mediated Assembly of Phenylboronic Acid Modified CdTe/ZnTe/ZnS Quantum Dots for Intracellular Glucose Probing. *Angew. Chem., Int. Ed.* **2010**, *49*, 6554−6558.
(27) Matsumoto, A.; Cabral, H.; Sato, N.; Kataoka, K.; Miyahara, Y. Assessment of Tumor Metastasis by the Direct Determination of Cell-Membrane Sialic Acid Expression. *Angew. Chem., Int. Ed.* **2010**, *49*, 5494−5497.
(28) Matsumoto, A.; Sato, N.; Kataoka, K.; Miyahara, Y. Noninvasive Sialic Acid Detection at Cell Membrane by Using Phenylboronic Acid Modified Self-Assembled Monolayer Gold Electrode. *J. Am. Chem. Soc.* **2009**, *31*, 12022−12023.
(29) Cao, J. T.; Hao, X. Y.; Zhu, Y. D.; Sun, K.; Zhu, J. J. Microfluidic Platform for the Evaluation of Multi-glycan Expressions on Living Cells Using Electrochemical Impedance Spectroscopy and Optical Microscope. *Anal. Chem.* **2012**, *84*, 6775−6782.
(30) Lizzi, A. R.; D'Alessandro, A. M.; Bozzi, A.; Cinque, B.; Oratore, A.; D'Andrea, G. Pattern Expression of Glycan Residues in AZT-Treated K562 Cells Analyzed by Lectin Cytochemistry. *Mol. Cell. Biochem.* **2007**, *300*, 29−37.

DOI: 10.1021/acsami.5b03519
ACS Appl. Mater. Interfaces 2015, 7, 14878−14884